

# Error Rate Analysis of Intelligent Reflecting Surfaces Aided Non-Orthogonal Multiple Access System

A. Vasuki<sup>1</sup> and Vijayakumar Ponnusamy<sup>2,\*</sup>

<sup>1</sup>Department of ECE, SRM Institute of Science and Technology, Vadapalani, Chennai, 600026, India

<sup>2</sup>Department of ECE, SRM Institute of Science and Technology, SRM Nagar, Kattankulathur, Chengalpattu, 603203, India

\*Corresponding Author: Vijayakumar Ponnusamy. Email: vijayakp@srmist.edu.in

Received: 12 August 2021; Accepted: 27 October 2021

**Abstract:** A good wireless device in a system needs high spectral efficiency. Non-Orthogonal Multiple Access (NOMA) is a technique used to enhance spectral efficiency, thereby allowing users to share information at the same time and same frequency. The information of the user is super-positioned either in the power or code domain. However, interference cancellation in NOMA aided system is challenging as it determines the reliability of the system in terms of Bit Error Rate (BER). BER is an essential performance parameter for any wireless network. Intelligent Reflecting Surfaces (IRS) enhances the BER of the users by controlling the electromagnetic wave propagation of a given channel. IRS is able to boost the Signal to Noise Ratio (SNR) at the receiver by introducing a phase shift in the incoming signal utilizing cost-effective reflecting materials. This paper evaluates users' error rate performance by utilizing IRS in NOMA. The error probability expression of users is derived under Rayleigh and Rician fading channel. The accuracy of derived analytical expressions is then validated via simulations. Impact of power allocation factor, coherent and random phase shifting of IRS is evaluated for the proposed IRS-NOMA system.

**Keywords:** NOMA; interference cancellation; bit error rate; signal to noise ratio

## 1 Introduction

The role of wireless communication systems has become inevitable across domains. The utility has increased with devices and various applications. Then, there is a need for massive connectivity with ultra-reliable and low latency among devices [1,2]. Appropriate techniques are developed and similar techniques are integrated into the Fifth generation (5G) wireless communication system to meet these requirements. This combined effect of technologies fulfills essential requirements, including high achievable rate, user fairness, energy efficiency, high spectral efficiency, low latency and achieving extremely low error rate within a wireless communication system [3,4]. To fulfill these demands of achieving enhanced spectral efficiency and low-latent transmission, Non-Orthogonal Multiple Access (NOMA) is utilized as a channel accessing mechanism in 5G and beyond cellular systems [5,6]. NOMA enables simultaneous transmission from multiple users to share their information by super-positioning



This work is licensed under a Creative Commons Attribution 4.0 International License, which permits unrestricted use, distribution, and reproduction in any medium, provided the original work is properly cited.

either on the power or code domain. In the power domain, different power levels are assigned for users based on the channel fading conditions. In case of two-user NOMA system, users are categorized as near user and far user. It is assumed that near user has better channel condition than far user. Therefore, near user is allocated with less power and far user with high power. NOMA differs from conventional OMA techniques wherein a single user alone is allowed to access resources in a given time or frequency. It's feasible with NOMA as it employs Successive Interference Cancellation (SIC) mechanism at the receiver to decode the user's information based on their power allocation order. SIC decodes the highest power signal and then detects the concerned user's signal, thereby canceling the user with the highest power allocation. Multiple users in the NOMA system can complicate the SIC mechanism. Accuracy in SIC decides the user's error rate at the receiving end.

With the evolution of integrated electronics [7], Intelligent Reflecting Surfaces (IRS) is a fabricated structure to make the complete wireless system intelligent [8]. IRS has been integrated with other technologies, which require a highly reliable and energy-efficient system. It interacts with the environment and enables constructive energy focusing on the users. The incident signal at IRS is reflected by an angle to achieve the energy focusing in the broadcast environment. The reflected signal is strengthened to extend the coverage area of the system. In recent times, many research works utilize the benefits of IRS and NOMA to accomplish the demands of the next-generation wireless communication system [9].

## **1.1 Related Works**

### *1.1.1 Error Rate Analysis for NOMA Systems*

In the research work [10], error rate performance of cooperative-NOMA network is analyzed. The expression of error probability is derived and the effect of power allocation on BER performance is analyzed. In [11], BER performance is investigated for two-user NOMA system with square Quadrature Amplitude Modulation (QAM) scheme. The authors of [12] consider the analysis of BER in downlink-NOMA system under Rayleigh fading channel for Binary Phase Shift Keying (BPSK) modulation scheme. The BER analysis of relay assisted NOMA system is considered in [13]. Pair-wise error probability expression is derived by considering Simultaneous Wireless Information Power Transfer (SWIPT). The exact expression of average BER for a two-user NOMA system is obtained for generalized frequency in the flat-fading channel [14]. In [15], BER performance for two-user NOMA system is analyzed by considering SIC for both uplink and downlink transmission. Similarly, the authors of [16] also address BER performance in downlink NOMA system with consideration of SIC errors. The average bit error probability is derived for Space-Shift-Keying (SSK)-NOMA system with three users in [17]. The error rate performance of cooperative Orthogonal Frequency Division Multiplexing (OFDM)-NOMA system with index modulation is investigated in [18]. The Maximum-Likelihood detector (ML) and greedy detector are considered for deriving the analytical expression of BER at the destination. The error probability of the OFDM-NOMA system is analyzed in [19] by considering Quadrature Phase Shift Keying (QPSK) modulation. The BER performance is analyzed over Rayleigh, Rician and Nakagami-m fading channels in [20] by using Minimum-Mean-Square-Error (MMSE) detector for downlink NOMA system.

### *1.1.2 Error Rate Analysis for IRS Aided Systems*

IRS is utilized for improving error rate performance in the wireless communication system. The research works of [21–23] analyze the error rate of IRS aided transmission. IRS acts as an access point as well as the reflector in [21]. Blind transmission (without knowing the environment) is assumed between the transmitter and users. Enhanced symbol error probability is achieved in IRS aided system. SNR performance of IRS aided wireless system is compared with massive MIMO in [22]. It also provides the relationship between

a number of array elements and SNR. It is stated that SNR in the IRS system varies nonlinearly with the number of reflective elements, wherein massive MIMO has linear variation. The closed-form bit error rate expression of IRS-NOMA is derived in [23], the number of reflecting elements in IRS is equally divided to enhance the signal propagation for the near and far user.

## 1.2 Contribution

Motivated by the above-mentioned recent works on NOMA and IRS, the proposed work considers NOMA-based wireless communication supported by IRS. The closed form expression of bit error probability in two-user downlink NOMA system is derived in [15]. Based on [15,21], the error probability of the two-user downlink IRS-NOMA system is derived in this paper. In the article [15], the near user signal is modulated using QPSK and BPSK modulation is used for far user. In this article, BPSK modulation is considered for both users. The main contributions of this article are

- Closed-form expressions of average error probability of received signal at IRS-NOMA are derived by considering SIC mechanism under Rayleigh and Rician fading channel.
- We consider Coherent and Random phase shifting at IRS and evaluate the BER performance of users.
- Optimum power allocation on BER performance is investigated in the proposed IRS-NOMA system.

## 1.3 Structure of the Paper

This article is organized as follows. IRS-NOMA system model is described in Section 2. In Section 3, the analytical expression of NOMA users is derived. The BER performance of the proposed IRS-NOMA system is discussed in Sections 4 and 5. The article is concluded in Section 6.

## 1.4 Notations

The detailed symbols and corresponding descriptions are listed in [Tab. 1](#).

**Table 1:** List of mathematical notations

Notation	Description
$\theta$	Phase shift matrix introduced at IRS
$\bar{P}_{1\text{Rayleigh}}(\epsilon), \bar{P}_{2\text{Rayleigh}}(\epsilon)$	Average error probability of $U_1$ and $U_2$ under Rayleigh fading channel
$\bar{P}_{1\text{Rician}}(\epsilon), \bar{P}_{2\text{Rician}}(\epsilon)$	Average error probability of $U_1$ and $U_2$ under Rician fading channel
$E[\cdot]$	Expectation operator
$f_{\gamma_{k\text{Rayleigh}}}(\gamma)$	PDF of the SNR $\gamma_k$ under Rayleigh fading
$f_{\gamma_{k\text{Rician}}}(\gamma)$	PDF of the SNR $\gamma_k$ under Rician fading
$I_0[\cdot]$	Modified bessel function
$M_{\gamma_{k\text{Rayleigh}}}$	Moment generating function of Rayleigh fading
$M_{\gamma_{k\text{Rician}}}$	Moment generating function of Rician fading
$h_{D1}$ and $h_{D2}$	Direct channel fading between BS- $U_1$ and BS- $U_2$
$g$	Channel fading between BS-IRS
$g_1$ and $g_2$	Channel fading between IRS- $U_1$ and IRS- $U_2$
$\text{Diag}(\cdot)$	Diagonal matrix
$C^{M \times N}$	$M \times N$ complex valued matrix
$(\cdot)^H$	Conjugate transpose

## 2 System Model for Proposed IRS Supported NOMA Communication

A downlink IRS-supported NOMA system is considered, as shown in Fig. 1. The proposed system consists of two users, IRS with  $N$  passive reflective elements and a Base Station (BS). In NOMA system, users are ordered and allocated with different power levels according to their average channel power. In the proposed two-user IRS-NOMA system, near user is termed as  $U_1$  and the far user is termed as  $U_2$ .

The power allocation ( $\alpha$ ) should satisfy the condition  $\sum_{i=1}^n \alpha_i = 1$  for  $n$ -user NOMA system. The far user is allocated with high power, wherein the near user with low power. In this proposed system, the BS transmits the superimposed signal from two different users with the power allocation of  $\alpha$  and  $(1 - \alpha)$ . The transmitted superimposed signal ( $x$ ) is given by

$$x = \sqrt{P_t \alpha} s_1 + \sqrt{P_t (1 - \alpha)} s_2 = \sqrt{a_1} s_1 + \sqrt{a_2} s_2 \quad (1)$$

where  $P_t$  and  $s_i$  ( $i = 1, 2$ ) denote the total transmit power and modulated symbols of users. The product terms  $P_t \alpha$  and  $P_t (1 - \alpha)$  are substituted as  $a_1$  and  $a_2$  for near and far users respectively.

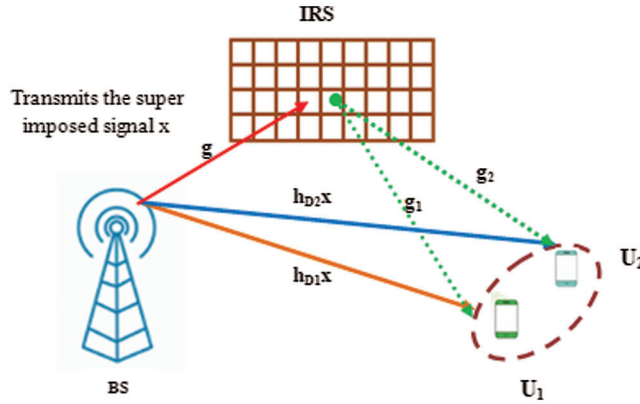


**Figure 1:** An illustration of IRS-NOMA aided transmission

### 2.1 Impact of IRS on Signal Transmission

In the system proposed, IRS is kept in between the BS and users to aid NOMA transmission. The users are assumed to receive a signal from BS and IRS. IRS is a reflecting array made up of periodic metasurfaces. Metasurfaces are artificially composite materials, which have been utilized in wireless communication for introducing considerable phase shift on the incident signal [24]. The array elements are termed as cell fabricated with PIN or varactor diode to introduce phase shift on the RF signal. The unusual characteristics of metamaterials in IRS make it to interrelate with both electric and magnetic fields of the input signal. The collective effect of array elements is utilized to focus the energy in the directions of users. As illustrated in Fig. 1, the IRS receives the incoming superimposed signal ( $x$ ) and introduces the phase shift of  $\theta$  on the reflected signal. The users in the focusing area can receive the reflected signal from IRS. The phase shift  $\theta$  can be tuned or adjusted to focus and de-focus the energy in the relevant and irrelevant directions.

### 2.2 Channel Fading

This paper assumes that the users receive direct signal as well as reflected signal. We analyze the IRS aided NOMA transmission in both Rayleigh as well as Rician fading. The direct channel fading coefficients between BS- $U_1$  and BS- $U_2$  are denoted as  $h_{D1}$  and  $h_{D2}$ . Let  $g$  denotes channel fading between BS and IRS,  $g_1$

and  $g_2$  be the channel coefficients between IRS and users ( $U_1, U_2$ ). Therefore, the received signals at the end-users ( $U_1, U_2$ ) are written as

$$y_1 = g^H \theta g_1 x + h_{D1}x + n_1 \quad (2)$$

$$y_2 = g^H \theta g_2 x + h_{D2}x + n_2 \quad (3)$$

where  $h_{D1}x$  and  $h_{D2}x$  represent the direct signal received at the users from BS.  $g^H \theta g_1 x$  and  $g^H \theta g_2 x$  represent received signals at  $U_1$  and  $U_2$  via BS-IRS–user channels.  $\theta$  is the phase shift matrix ( $N \times N$ ) introduced in the IRS to focus power towards users, which is given as diagonal matrix as  $\theta = \text{diag}\{\beta_1 e^{j\varphi_1}, \beta_2 e^{j\varphi_2}, \dots, \beta_N e^{j\varphi_N}\}$ ,  $\beta_i(0, 1)$ ,  $\varphi_i \in (0, \pi)$ .  $\beta_i$  and  $\varphi_i$  represent the amplitude of reflection and phase-shift at  $i^{\text{th}}$  reflecting unit of IRS. Fading coefficients of indirect channels (BS-IRS, IRS-users) are denoted by the vectors  $g \in C^{N \times 1}$ ,  $g_k \in C^{N \times 1}$  where ( $k=1, 2$ ). In the case of the Rician channel fading model, the fading coefficients  $h_{Dk}$ ,  $g$  and  $g_k$  are given by

$$h_{Dk} = \sqrt{\frac{K_1}{K_1+1}} \bar{h}_{Dk} + \sqrt{\frac{1}{K_1+1}} \tilde{h}_{Dk} \quad (4)$$

$$g = \sqrt{\frac{K_2}{K_2+1}} \bar{g} + \sqrt{\frac{1}{K_2+1}} \tilde{g} \quad (5)$$

$$g_k = \sqrt{\frac{K_3}{K_3+1}} \bar{g}_k + \sqrt{\frac{1}{K_3+1}} \tilde{g}_k \quad (6)$$

In (4),  $K_1$  is the Rician factor of  $h_{Dk}$ ,  $\bar{h}_{Dk}$  and  $\tilde{h}_{Dk}$  represent the dominant LoS and non-LoS (NLoS) terms.  $K_2$  is the Rician factor of  $g$ .  $\bar{g} \in C^{N \times 1}$  and  $\tilde{g} \in C^{N \times 1}$  indicates direct LoS component and NLoS terms. Similarly,  $K_3$  is the Rician factor of  $g_k$ .  $\bar{g}_k \in C^{N \times 1}$  and  $\tilde{g}_k \in C^{N \times 1}$  are the LoS component and NLoS terms. We assume that Maximal Ratio Combiner (MRC) [25] is employed to combine the direct and indirect signals at users. The channel is considered as the Additive White Gaussian Noise (AWGN), where  $n_i = N(0, \sigma_i^2)$  ( $i=1, 2$ ) and  $\sigma_i^2$  is noise variance. In case of NOMA-based communication, far user  $U_2$  decodes its information directly by considering other user's ( $U_1$ ) information as noise. The  $U_1$  (near user) applies SIC mechanism to decode its symbol  $s_1$ . First,  $U_1$  detects  $U_2$ , then subtracts the detected signal from the received superimposed signal  $y_1$  and then decodes its own signal.

### 2.3 Types of Phase-Shifting at IRS

Introduction of phase shift  $\theta$  at IRS can be coherent phase shifting and random phase shifting as mentioned in [21]. In the case of intelligent transmission, it is assumed that IRS has known the channel characteristics perfectly; the reflection angle  $\theta$  between IRS and users could be adjusted to maximize the received signal strength at the user. The IRS introduces phase shift randomly in the random phase-shifting method. In this paper, both phase-shifting methods are considered at IRS to evaluate the BER performance.

## 3 Performance Analysis

In this section, the average bit error probability of users ( $U_1$  and  $U_2$ ) in IRS-NOMA system is derived by assuming BPSK modulation for both the users under Rayleigh and Rician fading channel.

### 3.1 Average Error Probability of Far User Under Rayleigh Fading

For the BPSK modulation signal, the constellations of the received signal at  $U_1$  and  $U_2$  are as illustrated in Fig. 2.  $(b_1, b_2)$  represents the binary symbols of  $U_1$  and  $U_2$ . The ML detector [26] is employed to decode

the user symbols. The decision boundary depends on the amount of AWGN noise ( $n_i$ ) present in the received signal. For BPSK signal, decision boundary could be  $y_i > 0$  or  $y_i \leq 0$  ( $i = 1, 2$ ). The total error probability is calculated by summing up the error probability of every BPSK symbol multiplied by its prior probability. The prior probabilities of the superimposed signal in BPSK are  $\frac{1}{4}$ , since the probabilities of occurrence of all possible symbols ( $s_1, s_2$ ) are equal. In BPSK modulation, the in-phase component of noise influences the detection boundary [27]. The error in the detection occurs whenever the noise is higher than the signal. From the constellation diagram, the error probability  $U_2$  is expressed as  $P_2(e)$ ,

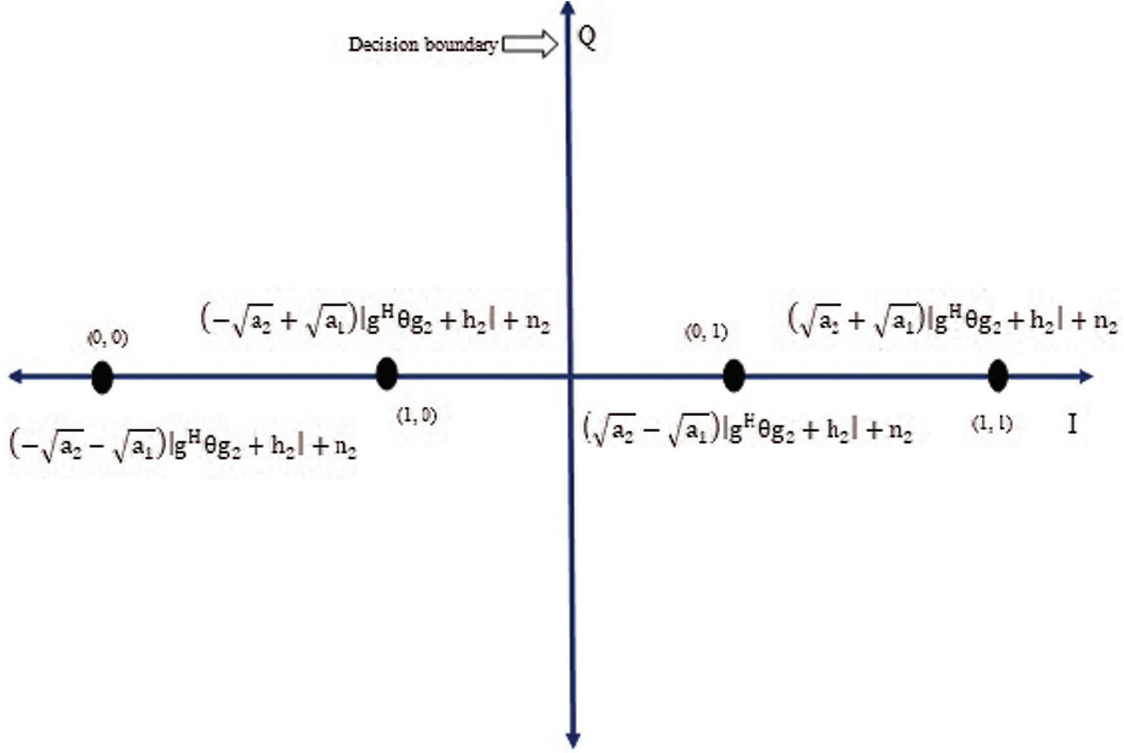


**Figure 2:** Signal constellation map for two-user IRS-NOMA system

$$P_2(e) = \frac{1}{2}pr(y_2 > 0 | b_2 = -1) + \frac{1}{2}pr(y_2 \leq 0 | b_2 = 1) \quad (7)$$

Using the ML detection principle, the conditional error probability is written as

$$P_2(e) = \frac{1}{2}pr(n_2 \geq (\sqrt{a_1} + \sqrt{a_2})(g^H \theta g_2 + h_{D2})) + \frac{1}{2}pr(n_2 \geq (\sqrt{a_2} - \sqrt{a_1})(g^H \theta g_2 + h_{D2})) \quad (8)$$

The error probability expressed in (8) can be written using complex Q-function [[28], Eq. (7.108)] with noise variance of  $\frac{N_0}{2}$ .

$$P_2(e) = \frac{1}{2} \left[ Q \left[ \frac{(\sqrt{a_1} + \sqrt{a_2})(g^H \theta g_2 + h_{D2})}{\sqrt{\frac{N_0}{2}}} \right] + Q \left[ \frac{(\sqrt{a_2} - \sqrt{a_1})(g^H \theta g_2 + h_{D2})}{\sqrt{\frac{N_0}{2}}} \right] \right] \quad (9)$$

Eq. (9) can be represented using instantaneous SNR as

$$\gamma_1 = \frac{2(\sqrt{a_1} + \sqrt{a_2})^2 |g^H \theta g_2 + h_{D2}|^2}{N_o}, \quad \bar{\gamma}_1 = \frac{2(\sqrt{a_1} + \sqrt{a_2})^2 E[|g^H \theta g_2 + h_{D2}|^2]}{N_o} \quad (10)$$

$$\gamma_2 = \frac{2(\sqrt{a_2} - \sqrt{a_1})^2 |g^H \theta g_2 + h_{D2}|^2}{N_o}, \quad \bar{\gamma}_2 = \frac{2(\sqrt{a_2} - \sqrt{a_1})^2 E[|g^H \theta g_2 + h_{D2}|^2]}{N_o} \quad (11)$$

In (10) and (11)  $\gamma_1$  and  $\gamma_2$  represent SNRs,  $\bar{\gamma}_1$  and  $\bar{\gamma}_2$  are the corresponding mean values. Where  $E[.]$  denotes the expectation operator. The expression (9) is rewritten in terms of SNR as

$$P_2(e) = \frac{1}{2} (Q(\sqrt{\gamma_1}) + Q(\sqrt{\gamma_2})) \quad (12)$$

Average error probability in AWGN over fading channel at far user is calculated by integrating the product of Gaussian Q-function and channel fading Probability Density Function (PDF)  $f_{\gamma_k}(\gamma_k)$ ,  $k=1, 2$  using [[29], Eq. (5.1)]

$$\bar{P}_2(e) = \frac{1}{2} \left[ \int_0^\infty Q(\sqrt{\gamma_1}) f_{\gamma_1 \text{Rayleigh}}(\gamma) d\gamma_1 + \int_0^\infty Q(\sqrt{\gamma_2}) f_{\gamma_2 \text{Rayleigh}}(\gamma) d\gamma_2 \right] \quad (13)$$

By substituting the Gaussian Q-function (10) can be rewritten using [[29], Eq. (5.2)]

$$\bar{P}_2(e) = \frac{1}{2} \left[ \frac{1}{\pi} \int_0^{\frac{\pi}{2}} \left\{ \int_0^\infty \exp\left(\frac{-\gamma_1}{2\sin^2\theta}\right) f_{\gamma_1 \text{Rayleigh}}(\gamma) d\gamma_1 \right\} d\theta + \frac{1}{\pi} \int_0^{\frac{\pi}{2}} \left\{ \int_0^\infty \exp\left(\frac{-\gamma_2}{2\sin^2\theta}\right) f_{\gamma_2 \text{Rayleigh}}(\gamma) d\gamma_2 \right\} d\theta \right] \quad (14)$$

where PDF of the SNRs for the Rayleigh distribution is given by [[29], Eq. (5.4)]

$$f_{\gamma_1 \text{Rayleigh}}(\gamma) = \frac{1}{\bar{\gamma}_1} e^{-\frac{\gamma}{\bar{\gamma}_1}} \quad (15)$$

$$f_{\gamma_2 \text{Rayleigh}}(\gamma) = \frac{1}{\bar{\gamma}_2} e^{-\frac{\gamma}{\bar{\gamma}_2}}, \quad \gamma \geq 0 \quad (16)$$

Using [[29], Eq. (5.3)], the term  $\left\{ \int_0^\infty \exp\left(\frac{-\gamma_k}{2\sin^2\theta}\right) f_{\gamma_k}(\gamma_k) d\gamma_k \right\}$ ,  $k=1, 2$  represents using Moment Generation Function (MGF) for the Rayleigh fading and (14) is expressed in terms of MGF as

$$\bar{P}_{2 \text{Rayleigh}}(e) = \frac{1}{2} \left[ \frac{1}{\pi} \int_0^{\frac{\pi}{2}} M_{\gamma_1 \text{Rayleigh}}\left(\frac{-1}{2\sin^2\theta}\right) d\theta + \frac{1}{\pi} \int_0^{\frac{\pi}{2}} M_{\gamma_2 \text{Rayleigh}}\left(\frac{-1}{2\sin^2\theta}\right) d\theta \right] \quad (17)$$

Using [[29], Eq. (5.5)],  $M_{\gamma_k \text{Rayleigh}}$   $k=1, 2$  for Rayleigh fading is expressed as

$$M_{\gamma_1 \text{Rayleigh}}(-s) = \frac{1}{1 + s\bar{\gamma}_1}, \quad M_{\gamma_2 \text{Rayleigh}}(-s) = \frac{1}{1 + s\bar{\gamma}_2} \quad (18)$$

where  $s = \frac{-1}{2\sin^2\theta}$  for BPSK modulation. With the use of [[29], Eq. (5.6)], by substituting (18) in (17), the error probability of far user becomes

$$\bar{P}_{2Rayleigh}(e) = \frac{1}{4} \left[ \left( 1 - \sqrt{\frac{\bar{\gamma}_1}{2 + \bar{\gamma}_1}} \right) + \left( 1 - \sqrt{\frac{\bar{\gamma}_2}{2 + \bar{\gamma}_2}} \right) \right] \quad (19)$$

### 3.2 Average Error Probability of Near User Under Rayleigh Fading

In NOMA system, the near user signal is decoded after canceling the far user information using SIC process. Far user information can be decoded correctly or erroneously during SIC process. Therefore, the error probability of near user is calculated as the sum of error probability under far user information decoded successfully and erroneously. The constellation map is shown in Fig. 3.

$$P_{1Rayleigh}(e) = P_1(e|U_{2successful}) + P_1(e|U_{2unsuccessful}) \quad (20)$$

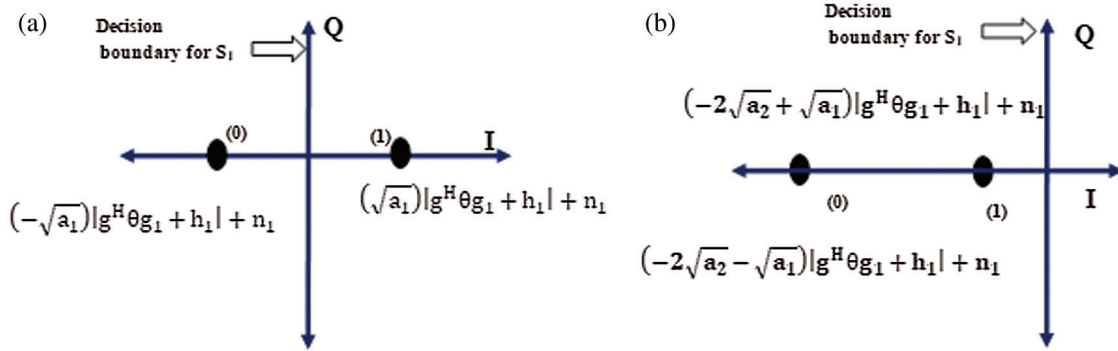


**Figure 3:** Signal constellation map for  $U_1$  signal detection (a) Decision boundary for  $U_1$  when  $U_2$  is detected successfully, (b) Decision boundary for  $U_1$  when  $U_2$  is detected unsuccessfully

In (20),  $P_1(e)$  represents the probability of error at  $U_1$ ,  $p_1(e|U_{2successful})$  indicates error probability of  $U_1$ , while  $U_2$  the signal is detected successfully.  $p_1(e|U_{2unsuccessful})$  represents error probability of  $U_1$ , when  $U_2$  signal is detected incorrectly. The constellation map of correct decoding and incorrect decoding of  $U_2$  is illustrated in Fig. 3.  $U_1$  signal is affected by channel fading and AWGN noise after SIC mechanism. During the detection of  $U_1$  symbol, the error probability of successful detection of  $U_2$  the symbol is considered as prior probability of different superimposed signals. Therefore,  $p_1(e|U_{2successful})$  is expressed as

$$P_1(e|U_{2successful}) = \frac{1}{2} \left\{ \begin{array}{l} \left[ \begin{array}{l} P_r(n_1 \leq (\sqrt{a_2} - \sqrt{a_1})(g^H \theta g_1 + h_{D1})) \\ P_r(n_1 \leq -\sqrt{a_1}(g^H \theta g_1 + h_{D1}) | n_1 \leq (\sqrt{a_2} - \sqrt{a_1})(g^H \theta g_1 + h_{D1})) \end{array} \right] + \\ \left[ \begin{array}{l} P_r(n_1 \leq (\sqrt{a_2} + \sqrt{a_1})(g^H \theta g_1 + h_{D1})) \\ P_r(n_1 \geq \sqrt{a_1}(g^H \theta g_1 + h_{D1}) | n_1 \leq (\sqrt{a_2} + \sqrt{a_1})(g^H \theta g_1 + h_{D1})) \end{array} \right] \end{array} \right\} \quad (21)$$

Using conditional probability of two events A and B,  $P(A|B) = \frac{P(A \cap B)}{P(B)}$ , (21) is written as,

$$P_1(e|U_{2successful}) = \frac{1}{2} \left\{ \begin{array}{l} P_r(n_1 \leq -\sqrt{a_1}(g^H \theta g_1 + h_{D1})) + \\ P_r(\sqrt{a_1}(g^H \theta g_1 + h_{D1}) \leq n_1 \leq (\sqrt{a_2} + \sqrt{a_1})(g^H \theta g_1 + h_{D1})) \end{array} \right\} \quad (22)$$

The first term  $P_r(n_1 \leq -\sqrt{a_1}(g^H \theta g_1 + h_{D1}))$  and second terms  $P_r(\sqrt{a_1}(g^H \theta g_1 + h_{D1}) \leq n_1 \leq (\sqrt{a_2} + \sqrt{a_1})(g^H \theta g_1 + h_{D1}))$  of (22) can be represented in Q-function as

$$P_r(n_1 \leq -\sqrt{a_1}(g^H \theta g_1 + h_{D1})) = Q(\sqrt{\gamma_3}) \quad (23)$$

$$P_r(\sqrt{a_1}(g^H \theta g_1 + h_{D1}) \leq n_1 \leq (\sqrt{a_2} + \sqrt{a_1})(g^H \theta g_1 + h_{D1})) = Q(\sqrt{\gamma_3}) - Q(\sqrt{\gamma_4}) \quad (24)$$

where,  $\gamma_3 = \frac{2(\sqrt{a_1})^2 |g^H \theta g_1 + h_{D1}|^2}{N_o}$ ,  $\gamma_4 = \frac{2(\sqrt{a_1} + \sqrt{a_2})^2 |g^H \theta g_1 + h_{D1}|^2}{N_o}$  and the mean values are  $\bar{\gamma}_3 = \frac{2(\sqrt{a_1})^2 E[|g^H \theta g_1 + h_{D1}|^2]}{N_o}$ ,  $\bar{\gamma}_4 = \frac{2(\sqrt{a_1} + \sqrt{a_2})^2 E[|g^H \theta g_1 + h_{D1}|^2]}{N_o}$ .

Therefore error probability of  $U_1$  when  $s_2$  detected correctly is calculated by substituting (23) and (24) in (22) as

$$P_1(e|U_2 \text{ successful}) = \frac{1}{2} [2Q(\sqrt{\gamma_3}) - Q(\sqrt{\gamma_4})] \quad (25)$$

In case of incorrect detection of  $s_2$ , this is shown in Fig. 3b. When the symbol  $b_2 = 1$  is transmitted for  $U_2$  and is decoded as  $b_2 = -1$ . Thus, the error probability of symbol  $s_1$  at  $U_1$  is calculated by taking the product of the error probability of every symbol in the constellation map shown in Fig. 3b. with respective prior error probability of  $U_2$  symbol. From the constellation map,  $p_1(e|U_2 \text{ unsuccessful})$  is expressed as

$$P_1(e|U_2 \text{ unsuccessful}) = \frac{1}{2} \left\{ \begin{array}{l} \left[ \begin{array}{l} P_r(n_1 \geq (\sqrt{a_2} - \sqrt{a_1})(g^H \theta g_1 + h_{D1})) \\ P_r(n_1 \leq (2\sqrt{a_2} - \sqrt{a_1})(g^H \theta g_1 + h_{D1}) | n_1 \geq (\sqrt{a_2} - \sqrt{a_1})(g^H \theta g_1 + h_{D1})) \end{array} \right] + \\ \left[ \begin{array}{l} P_r(n_1 \geq (\sqrt{a_2} + \sqrt{a_1})(g^H \theta g_1 + h_{D1})) \\ P_r(n_1 \geq (2\sqrt{a_2} + \sqrt{a_1})(g^H \theta g_1 + h_{D1}) | n_1 \geq (\sqrt{a_2} + \sqrt{a_1})(g^H \theta g_1 + h_{D1})) \end{array} \right] \end{array} \right\} \quad (26)$$

$P_1(e|U_2 \text{ unsuccessful})$  in (26) is rewritten using ML principle as

$$P_1(e|U_2 \text{ unsuccessful}) = \frac{1}{2} \left\{ \left[ \begin{array}{l} P_r((\sqrt{a_2} - \sqrt{a_1})(g^H \theta g_1 + h_{D1}) \leq n_1 \leq (2\sqrt{a_2} - \sqrt{a_1})(g^H \theta g_1 + h_{D1})) + \\ P_r(n_1 \geq (2\sqrt{a_2} + \sqrt{a_1})(g^H \theta g_1 + h_{D1})) \end{array} \right] \right\} \quad (27)$$

The first  $P_r((\sqrt{a_2} - \sqrt{a_1})(g^H \theta g_1 + h_{D1}) \leq n_1 \leq (2\sqrt{a_2} - \sqrt{a_1})(g^H \theta g_1 + h_{D1}))$  and second term  $P_r(n_1 \geq (2\sqrt{a_2} + \sqrt{a_1})(g^H \theta g_1 + h_{D1}))$  of (27) are expressed in terms of Q-function as

$$P_r((\sqrt{a_2} - \sqrt{a_1})(g^H \theta g_1 + h_{D1}) \leq n_1 \leq (2\sqrt{a_2} - \sqrt{a_1})(g^H \theta g_1 + h_{D1})) = Q(\sqrt{\gamma_5}) - Q(\sqrt{\gamma_6}) \quad (28)$$

$$P_r(n_1 \geq (2\sqrt{a_2} + \sqrt{a_1})(g^H \theta g_1 + h_{D1})) = Q(\sqrt{\gamma_7}) \quad (29)$$

where  $\gamma_5 = \frac{2(\sqrt{a_2} - \sqrt{a_1})^2 |g^H \theta g_1 + h_{D1}|^2}{N_o}$ ,  $\gamma_6 = \frac{2(2\sqrt{a_2} - \sqrt{a_1})^2 |g^H \theta g_1 + h_{D1}|^2}{N_o}$ ,  $\gamma_7 = \frac{2(2\sqrt{a_2} + \sqrt{a_1})^2 |g^H \theta g_1 + h_{D1}|^2}{N_o}$  and their corresponding mean expressions are  $\bar{\gamma}_5 = \frac{2(\sqrt{a_2} - \sqrt{a_1})^2 E[|g^H \theta g_1 + h_{D1}|^2]}{N_o}$ ,  $\bar{\gamma}_6 = \frac{2(2\sqrt{a_2} - \sqrt{a_1})^2 E[|g^H \theta g_1 + h_{D1}|^2]}{N_o}$ ,  $\bar{\gamma}_7 = \frac{2(2\sqrt{a_2} + \sqrt{a_1})^2 E[|g^H \theta g_1 + h_{D1}|^2]}{N_o}$

By substituting (28) and (29) in (27),  $P_1(e|U_2 \text{ unsuccessful})$  is written as

$$p_1(e|U_2 \text{ unsuccessful}) = \frac{1}{2} [Q(\sqrt{\gamma_5}) + Q(\sqrt{\gamma_7}) - Q(\sqrt{\gamma_6})] \quad (30)$$

By combining (25) and (30) and using (13), (14), (17) and (18) the probability of error for near user  $U_1$  signal is written using as,

$$\bar{P}_{1\text{Rayleigh}}(e) = \frac{1}{2} \left( 1 - \sqrt{\frac{\bar{\gamma}_3}{2 + \bar{\gamma}_3}} \right) + \frac{1}{4} \left[ \sqrt{\frac{\bar{\gamma}_4}{2 + \bar{\gamma}_4}} - \sqrt{\frac{\bar{\gamma}_5}{2 + \bar{\gamma}_5}} + \sqrt{\frac{\bar{\gamma}_6}{2 + \bar{\gamma}_6}} - \sqrt{\frac{\bar{\gamma}_7}{2 + \bar{\gamma}_7}} \right] \quad (31)$$

### 3.3 Average Error Probability of Far User Under Rician Fading

The average error probability of far users under the Rician fading channel is derived by substituting the PDF and MGF of Rician distribution in (14). Where PDF of Rician fading is expressed using [[29], Eq. (5.10)]

$$f_{\gamma_{kRician}}(\gamma) = \frac{(1+K)}{\bar{\gamma}_k} e^{-K} \exp\left[-\frac{(1+K)\gamma_k}{\bar{\gamma}_k}\right] I_0\left[2\sqrt{K}\sqrt{\frac{(1+K)\gamma_k}{\bar{\gamma}_k}}\right], \quad k = 1, 2 \quad (32)$$

where  $I_0[\cdot]$  represents the modified Bessel function. Similarly, the MGF of Rician fading using [[29], Eq. (5.11)] is represented by

$$M_{\gamma_{kRician}}(-s) = \frac{(1+K)}{1+K+s\bar{\gamma}_k} \exp\left[\frac{-Ks\bar{\gamma}_k}{1+K+s\bar{\gamma}_k}\right], \quad s > 0, \quad k = 1, 2 \quad (33)$$

By substituting alternate representation of MGF for Rician fading in (17), the average error probability of far user is expressed as

$$\bar{P}_2(e) = \frac{1}{2} \left[ \frac{1}{\pi} \int_0^{\frac{\pi}{2}} M_{\gamma_{1Rician}}\left(\frac{-1}{2\sin^2\theta}\right) d\theta + \frac{1}{\pi} \int_0^{\frac{\pi}{2}} M_{\gamma_{2Rician}}\left(\frac{-1}{2\sin^2\theta}\right) d\theta \right] \quad (34)$$

Therefore by substituting (34), the average error probability for the far user under Rician fading can be expressed as

$$\bar{P}_{2Rician}(e) = \frac{1}{2} \left\{ \begin{aligned} & \frac{1}{\pi} \int_0^{\frac{\pi}{2}} \frac{(1+K)\sin^2\theta}{(1+K)\sin^2\theta + \bar{\gamma}_1} \exp\left[\frac{-K\bar{\gamma}_1}{(1+K)\sin^2\theta + \bar{\gamma}_1}\right] d\theta + \\ & \frac{1}{\pi} \int_0^{\frac{\pi}{2}} \frac{(1+K)\sin^2\theta}{(1+K)\sin^2\theta + \bar{\gamma}_2} \exp\left[\frac{-K\bar{\gamma}_2}{(1+K)\sin^2\theta + \bar{\gamma}_2}\right] d\theta \end{aligned} \right\} \quad (35)$$

### 3.4 Average Error Probability of Near User Under Rician Fading

Similarly, the error probability of successful detection of  $U_2$  signal at near user under Rician fading can be expressed by introducing (32) and (33) in (25)

$$\bar{P}_{1(e|U_2\text{successful})Rician}(e) = \frac{1}{2} \left\{ \begin{aligned} & \frac{2}{\pi} \int_0^{\frac{\pi}{2}} \frac{(1+K)\sin^2\theta}{(1+K)\sin^2\theta + \bar{\gamma}_3} \exp\left[\frac{-K\bar{\gamma}_3}{(1+K)\sin^2\theta + \bar{\gamma}_3}\right] d\theta - \\ & \frac{1}{\pi} \int_0^{\frac{\pi}{2}} \frac{(1+K)\sin^2\theta}{(1+K)\sin^2\theta + \bar{\gamma}_4} \exp\left[\frac{-K\bar{\gamma}_4}{(1+K)\sin^2\theta + \bar{\gamma}_4}\right] d\theta \end{aligned} \right\} \quad (36)$$

The error probability of unsuccessful detection of  $U_2$  signal at near user for Rician fading is expressed by rewriting (30)

$$\bar{P}_{1(e|U_2\text{unsuccessful})Rician}(e) = \frac{1}{2} \left\{ \begin{array}{l} \frac{1}{\pi} \int_0^{\frac{\pi}{2}} \frac{(1+K)\sin^2\theta}{(1+K)\sin^2\theta + \bar{\gamma}_5} \exp\left[\frac{-K\bar{\gamma}_5}{(1+K)\sin^2\theta + \bar{\gamma}_5}\right] d\theta - \\ \frac{1}{\pi} \int_0^{\frac{\pi}{2}} \frac{(1+K)\sin^2\theta}{(1+K)\sin^2\theta + \bar{\gamma}_6} \exp\left[\frac{-K\bar{\gamma}_6}{(1+K)\sin^2\theta + \bar{\gamma}_6}\right] d\theta + \\ \frac{1}{\pi} \int_0^{\frac{\pi}{2}} \frac{(1+K)\sin^2\theta}{(1+K)\sin^2\theta + \bar{\gamma}_7} \exp\left[\frac{-K\bar{\gamma}_7}{(1+K)\sin^2\theta + \bar{\gamma}_7}\right] d\theta \end{array} \right\} \quad (37)$$

Thus the total average error probability at  $U_1$  under Rician fading is calculated by summing (36) and (37)

$$\bar{P}_{1Rician}(e) = \bar{P}_{1(e|U_2\text{successful})Rician}(e) + \bar{P}_{1(e|U_2\text{unsuccessful})Rician}(e) \quad (38)$$

#### 4 Simulation Results

In this section, we analyze the error probability expressions of near and far user numerically and verify the results via simulations. The simulation parameters are listed in Tab. 2.

**Table 2:** Simulation parameters

Parameters	Type
Channel	AWGN
Modulation	BPSK
Power allocation for users	$\alpha = 0.2$ ( $U_1$ ), $\alpha=0.8$ ( $U_2$ )
Number of transmitted bits	$10^6$
Fading channel	Rayleigh and Rician fading
Number of passive reflecting elements	32
Rician factors	$K_1, K_2, K_3 = 10$
Distance between BS- $U_1$ , BS- $U_2$	1.5, 5 m
Distance between BS-IRS	1 m
Distance between IRS- $U_1$ , IRS- $U_2$	1, 3 m
Pathloss exponent ( $\gamma$ )	1.6

##### 4.1 Theoretical BER Evaluation of Proposed Method with Coherent Phase Shifting

In the simulation results, near and far users are denoted as  $U_1$  and  $U_2$ . The IRS-NOMA transmission is investigated at an indoor environment model [30] with a path loss exponent of 1.6. Far user is allocated with the factor of  $\alpha=0.8$ , wherein near user with  $\alpha=0.2$ . The derived analytical expressions for Rayleigh [(19) and (31)] and Rician fading [(35) and (38)] channel are verified via simulations as shown in Figs. 4a and 4b. The simulation results show the accuracy of the derived expression. We also compare the performance of the derived BER expressions of the proposed two-user IRS-NOMA system with simulation results.

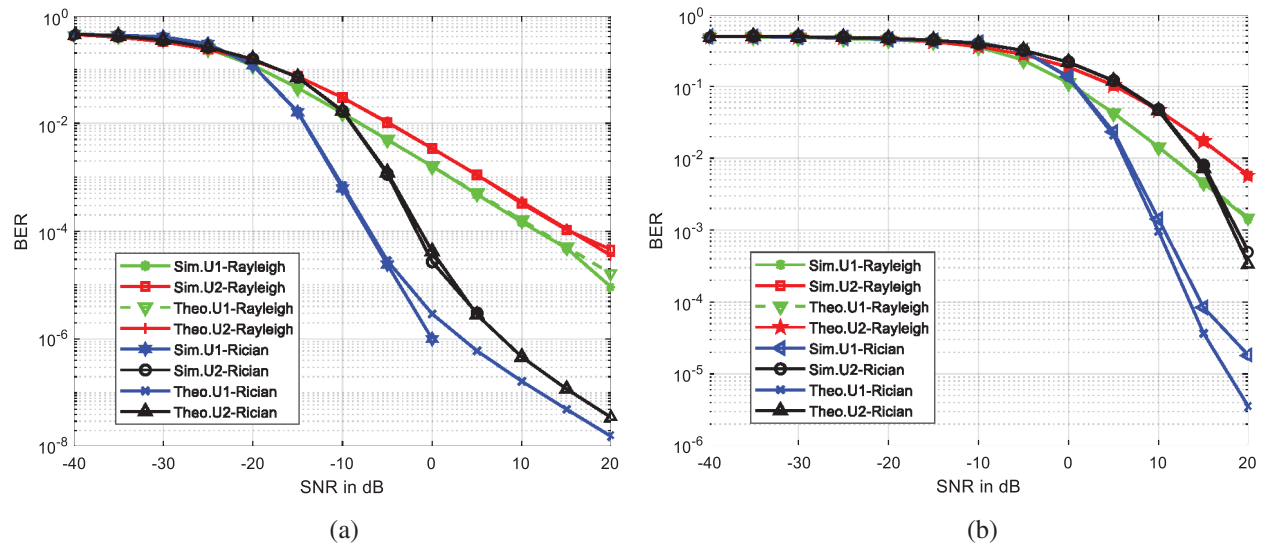


**Figure 4:** Performance verification of derived expressions under Rayleigh and Rician channel (a) coherent phase shifting, (b) random phase shifting

#### 4.2 Theoretical BER Evaluation of Proposed Method with Random Phase Shifting

Fig. 4b illustrates the analytical BER performance of the IRS-NOMA system with random phase shifting at IRS under Rayleigh and Rician fading. It has been shown that the BER of users at coherent phase-shifting outperforms the random phase-shifting method in low SNR regions.

#### 4.3 Performance Comparison Between NOMA and IRS Aided NOMA System

The impact of IRS in the NOMA system is evaluated as shown in Fig. 5, it has been demonstrated that BER performance of IRS aided NOMA system outperforms the conventional NOMA system under both fading channels. The proposed IRS-NOMA system achieves an approximate 30 dB SNR gain to obtain  $10^{-3}$  BER than NOMA system for both users from the simulation results. From the simulation analysis, the proposed IRS-NOMA outperforms NOMA, especially in the low SNR region. While comparing the BER-performance of the proposed IRS-NOMA system with the conventional NOMA system in [15], the former has a gain of 30 dB SNR at BER of  $10^{-3}$  under Rayleigh fading channel. Wherein [15] considers QPSK modulation for near users and BPSK for far users. The performance comparison between the proposed IRS-NOMA system with reference to NOMA system [[15], Fig. 4a] is listed in Tab. 3. It has been shown that introducing IRS in NOMA system enhances the BER performance considerably than NOMA system. The proposed simulation work as shown in Fig. 5 is obtained by considering BPSK modulation for both users with the pathloss exponent of 1.6 and 32 number of reflective elements in IRS under Rayleigh fading channel.

#### 4.4 Effect of Power Allocation Factor on IRS-NOMA System Under Rayleigh and Rician Fading

The effect of power allocation on BER performance of IRS-NOMA system is investigated and illustrated as shown in Fig. 6. The variations of BER performance with power allocation for various transmit SNR are analyzed and illustrated as shown in Fig. 7. In case of  $U_1$ , though the power allocation is increased, the BER performance is limited because of SIC process. The better BER performance is achieved at  $\alpha = 0.25$  with the transmit SNR of  $-10$  dB under both fading channels.

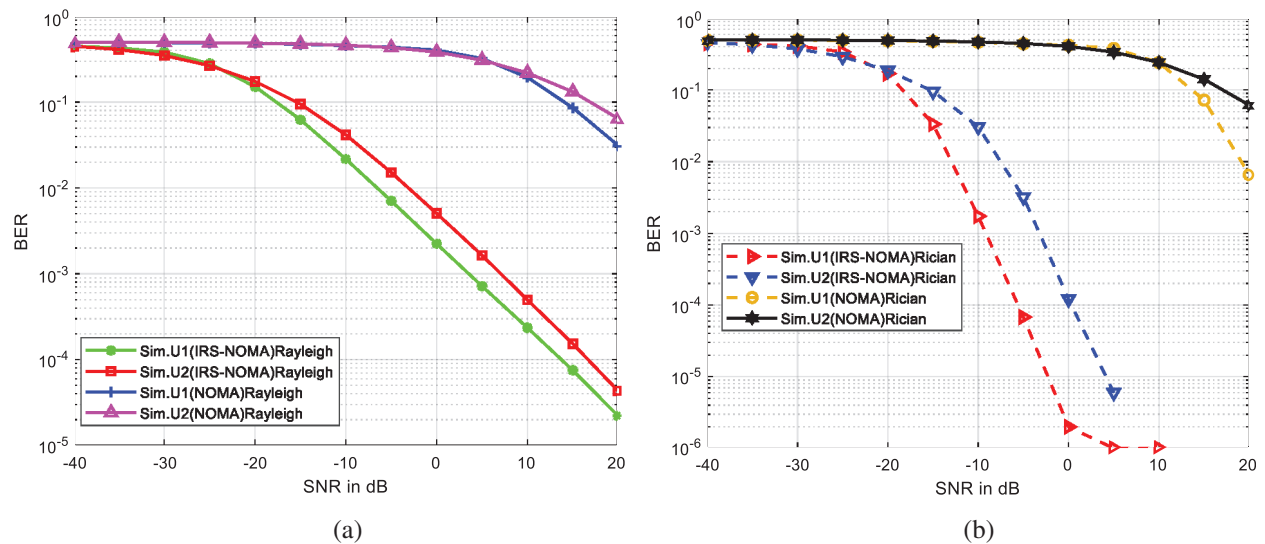


**Figure 5:** BER comparison between IRS-NOMA and conventional NOMA system (a) Rayleigh fading, (b) Rician fading

**Table 3:** BER Performance comparison of IRS-NOMA and NOMA system

Target BER	User	Required transmit SNR(dB)- NOMA [13]	Required transmit SNR(dB)- IRS-NOMA
$10^{-1}$	$U_1$	10	-20
	$U_2$	10	-15
$10^{-2}$	$U_1$	22	-8
	$U_2$	24	-5
$10^{-3}$	$U_1$	33	3
	$U_2$	35	8
$10^{-4}$	$U_1$	40	12
	$U_2$	40	15

## 5 Discussion

In the simulation results, both Rayleigh and Rician channel fading are considered. Rician distribution has dominant LoS component, therefore the performance of Rician channel is better than Rayleigh channel. In Rician fading BER of  $10^{-3}$  is obtained with 10 dB lesser SNR compared to Rayleigh fading channel as illustrated in Fig. 4a. Similarly, the random phase-shifting method requires 20 dB more SNR than coherent phase shifting to achieve the particular BER as shown in Fig. 4b.

As shown in Fig. 6, effect of power allocation also influences the performance of IRS-NOMA system. Under Rayleigh fading, the BER performance of  $U_2$  is better at power allocation  $\alpha = 0.55$ , it achieves 2 dB SNR gain to reach the BER of  $10^{-3}$  than power allocation of  $\alpha = 0.8$ . In the case of  $U_1$ , the better performance is obtained at  $\alpha = 0.2$ . In case of Rician fading, a 5 dB SNR gain is obtained for far users at  $\alpha = 0.55$  than  $\alpha = 0.8$ . The proposed work is analyzed for an indoor environment; the optimum number of reflective elements with appropriate power allocation factor decides the performance of the proposed system.

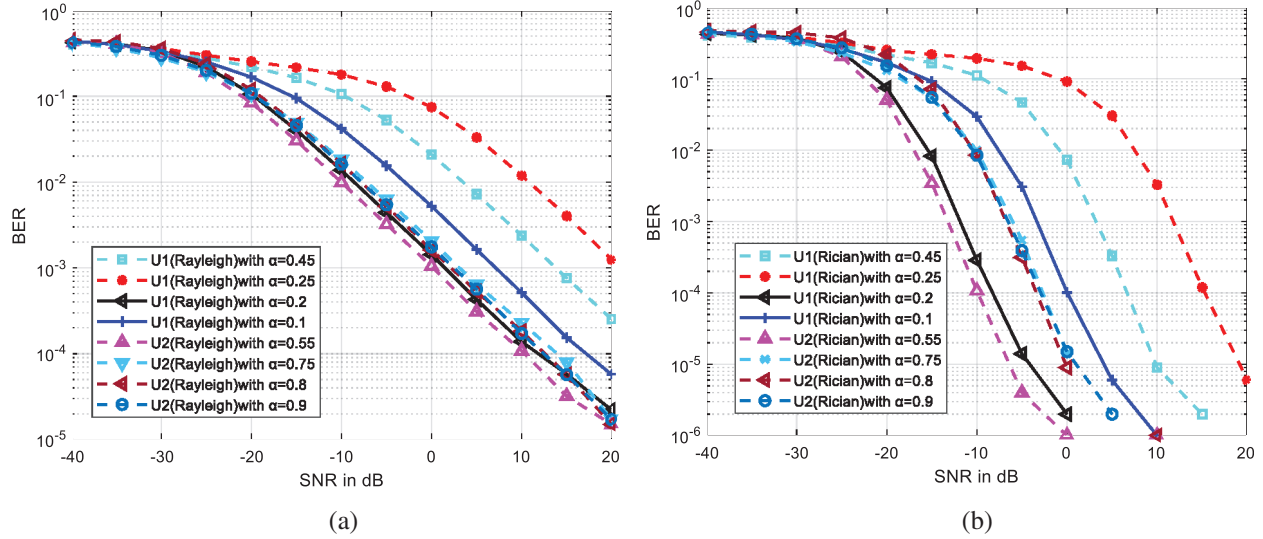


**Figure 6:** BER performance evaluation for different power allocation factors (a) Rayleigh fading, (b) Rician fading

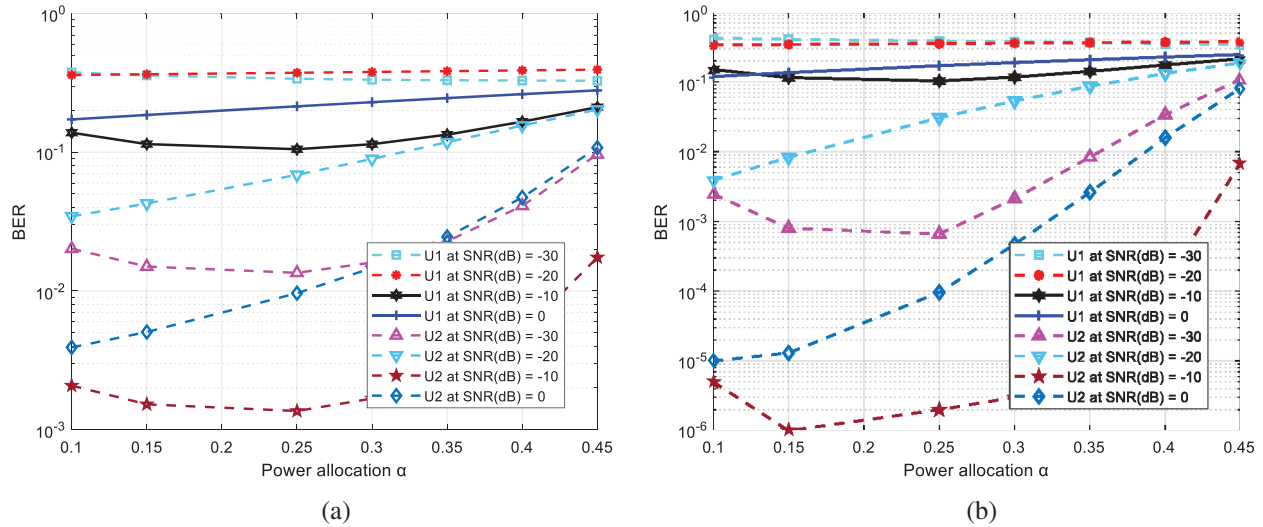


**Figure 7:** Impact of power allocation on BER performance for different SNR (a) Rayleigh fading, (b) Rician fading

## 6 Conclusion

In this paper, we derive the closed-form error probability expressions for two-user downlink NOMA system by considering SIC over Rayleigh and Rician fading channel. We consider random and coherent phase shifting at IRS. Based on the simulation results, we analyze performance comparison between IRS aided NOMA and NOMA systems. Our objective is to improve the error rate performance of the proposed system considering the practical SIC method. From the evaluation results, the proposed IRS-NOMA outperforms NOMA in the low SNR region. We evaluate the effect of the number of reflective elements on BER performance. The proposed system is analyzed by considering the simulation set up of indoor pathloss model with minimum pathloss. We have considered the fixed distance among the devices.

The proper placement of IRS could be explored. The simulation results are obtained with 32 number of reflecting elements at IRS. The power consumption of the passive reflecting elements will be considered for evaluation in the future. In the future, we optimize the IRS parameters to further enhance the performance of the proposed IRS-NOMA system.

**Funding Statement:** The authors received no specific funding for this study.

**Conflicts of Interest:** The authors declare that they have no conflicts of interest to report regarding the present study.

## References

- [1] G. Wunder, P. Jung, M. Kasparick, T. Wild, F. Schaich *et al.*, "5GNOW: Non-orthogonal, asynchronous waveforms for future mobile applications," *IEEE Communications Magazine*, vol. 52, no. 2, pp. 97–105, 2014.
- [2] P. Vijayakumar, J. George, S. Malarvizhi and A. Sriram, "Analysis and implementation of reliable spectrum sensing in OFDM based cognitive radio," in *Smart Computing and Informatics, Smart Innovation, Systems and Technologies*, Singapore: Springer, pp. 565–572, 2017.
- [3] J. G. Andrews, S. Buzzi and W. Choi, "What will 5G be?," *IEEE Journal on Selected Areas in Communications*, vol. 32, no. 6, pp. 1065–1082, 2014.
- [4] P. Vijayakumar and S. Malarvizhi, "Hardware impairment detection and prewhitening on MIMO precoder for spectrum sharing," *Wireless Personal Communications*, vol. 96, no. 1, pp. 1557–1576, 2017.
- [5] Y. Saito, Y. Kishiyama, A. Benjebbour, T. Nakamura, A. Li *et al.*, "Non-orthogonal multiple access (NOMA) for cellular future radio access," in *2013 IEEE 77th Vehicular Technology Conf. (VTC Spring)*, Dresden, Germany, pp. 1–5, 2013.
- [6] Z. Ding, Z. Yang, P. Fan and H. V. Poor, "On the performance of non-orthogonal multiple access in 5G systems with randomly deployed users," *IEEE Signal Proc. Letters*, vol. 21, no. 12, pp. 1501–1505, 2014.
- [7] P. Vijayakumar and S. Malarvizhi, "Wide band full-duplex spectrum sensing with self-interference cancellation—an efficient sdr implementation," *Mobile Networks and Applications*, vol. 22, no. 4, pp. 702–711, 2017.
- [8] S. Hu, F. Rusek and O. Edfors, "Beyond massive MIMO: The potential of data transmission with large intelligent surfaces," *IEEE Transactions on Signal Processing*, vol. 66, no. 10, pp. 2746–2748, 2018.
- [9] X. Yu, D. Xu and R. Schober, "MISO wireless communication systems via intelligent reflecting surfaces," in *IEEE/CIC Int. Conf. on Communications in China (ICCC)*, Changchun, China, pp. 735–740, 2019.
- [10] F. Kara and H. Kaya, "On the error performance of cooperative-NOMA with statistical CSIT," *IEEE Communications Letters*, vol. 23, no. 1, pp. 128–131, 2019.
- [11] T. Assaf, A. J. Al-Dweik, M. S. E. Moursi, H. Zeineldin and M. Al-Jarrah, "Exact Bit error-rate analysis of Two-user NOMA using QAM with arbitrary modulation orders," *IEEE Communications Letters*, vol. 24, no. 12, pp. 2705–2709, 2020.
- [12] M. Aldababsa, C. Goztepe, G. K. Kurt and O. Kucur, "Bit error rate for NOMA network," *IEEE Communications Letters*, vol. 24, no. 6, pp. 1188–1191, 2020.
- [13] L. Bariah, S. Muhaidat and A. Al-Dweik, "Error probability analysis of NOMA-based relay networks with SWIPT," *IEEE Communications Letters*, vol. 23, no. 7, pp. 1223–1226, 2019.
- [14] A. S. Alqahtani and E. Alsusa, "Performance analysis of downlink NOMA system over  $\alpha$ - $\eta$ - $\mu$  generalized fading channel," in *2020 IEEE 91st Vehicular Technology Conf. (VTC2020-Spring)*, Antwerp, Belgium, pp. 1–5, 2020.
- [15] F. Kara and H. Kaya, "BER performances of downlink and uplink NOMA in the presence of SIC errors over fading channels," *IET Communications*, vol. 12, no. 15, pp. 1834–1844, 2018.
- [16] J. Monika, S. Sandhya, S. Nikhil and R. Divyang, "Performance analysis at far and near user in NOMA based system in presence of SIC error," *International Journal of Electronics and Communications*, vol. 114, no. 19, pp. 1–16, 2019.
- [17] F. Kara and H. Kaya, "Performance analysis of SSK-NOMA," *IEEE Transactions on Vehicular Technology*, vol. 68, no. 7, pp. 6231–6242, 2019.

- [18] X. Chen, M. Wen and S. Dang, "On the performance of cooperative OFDM-NOMA system with index modulation," *IEEE Wireless Communications Letters*, vol. 9, no. 9, pp. 1346–1350, 2020.
- [19] H. S. Ghazi and K. W. Wesolowski, "Improved detection in successive interference cancellation NOMA OFDM receiver," *IEEE Access*, vol. 7, no. 9, pp. 103325–103335, 2019.
- [20] A. Vasuki and P. Vijayakumar, "Analysis of error rate for NOMA system different fading channel," in *1st Int. Conf. on Mathematical Techniques and Applications, AIP Conf. Proc.*, Chennai, India, pp. 1–6, 2020.
- [21] E. Basar, "Transmission through large intelligent surfaces: A New frontier in wireless communications," in *European Conf. on Networks and Communications*, Valencia, Spain, pp. 112–117, 2019.
- [22] J. Ye, S. Guo and M. S. Alouini, "Joint reflecting and precoding designs for SER minimization in reconfigurable intelligent surfaces assisted MIMO systems," *IEEE Transactions on Wireless Communications*, vol. 19, no. 8, pp. 5561–5574, 2020.
- [23] V. C. Thirumavalavan and T. S. Jayaraman, "BER analysis of reconfigurable intelligent surface assisted downlink power domain NOMA system," in *2020 Int. Conf. on COMMunication Systems & NETWORKS (COMSNETS)*, Bengaluru, India, pp. 519–522, 2020.
- [24] H. Yang, X. Cao, F. Yang, J. Gao, S. Xu *et al.*, "A programmable metasurface with dynamic polarization, scattering and focusing control," *Scientific Reports*, vol. 6, no. 1, pp. 1–11, 2016.
- [25] R. Liu, A. K. Sadek, W. Su and A. Kwasinski, "Introduction," in *Cooperative Communications and Networking*, 1<sup>st</sup> ed., New York, Cambridge University Press, pp. 3–42, 2009.
- [26] E. Caliskan, A. Maatouk, M. Koca, M. Assaad, G. Gui *et al.*, "A simple NOMA scheme with optimum detection," in *2018 IEEE Global Communications Conf. (GLOBECOM)*, Abu Dhabi, United Arab Emirates, pp. 1–6, 2018.
- [27] J. W. Craig, "A new, simple and exact result for calculating the probability of error for two-dimensional signal constellations," in *MILCOM 91-Conf. Record*, McLean, VA, USA, pp. 571–575, 1991.
- [28] S. Haykin, "Signaling over AWGN Channels," in *Digital Communication Systems*, 1<sup>st</sup> ed., vol. 1, New York: John Wiley & Sons, Inc., pp. 323–444, 2004.
- [29] M. K. Simon and M. S. Alouini, "Useful expressions for evaluating average error probability performance," in *Digital Communication Over Fading Channels*, 1<sup>st</sup> ed., vol. 1, New York: John Wiley & Sons, Inc., pp. 99–139, 2000.
- [30] A. Goldsmith, "Pathloss and Shadowing," in *Wireless Communications*, 1<sup>st</sup> ed., vol. 1, New York: Cambridge University Press, pp. 27–60, 2005.